# In Silico Modeling and Validation of the Effect of Calcium-Activated Potassium Current on Ventricular Repolarization in Failing Myocytes

Marta Gómez, Jesús Carro, Esther Pueyo, Alba Pérez, Aída Oliván and Violeta Monasterio

***Abstract*— Objective: The pathophysiological role of the small conductance calcium-activated potassium (SK) channels in human ventricular myocytes remains unclear. Experimental studies have reported upregulation of SK channels in pathological states, potentially contributing to ventricular repolarization. In heart failure (HF) patients, this upregulation could be an adaptive physiological response to shorten the action potential duration (APD) under conditions of reduced repolarization reserve. This work aimed to uncover the contribution of SK channels to ventricular repolarization in failing myocytes. Methods: We extended an in silico electrophysiological model of human ventricular failing myocytes by including SK channel activity. To calibrate the maximal SK current conductance ($G_{SK}$), we simulated action potentials (APs) at different pacing frequencies and matched the AP duration changes induced by SK channel inhibition or activation to different available experimental data from human failing ventricles for adjustment. Results: The optimal value obtained for $G_{SK}$ was 4.288 $\mu$S/$\mu$F in mid-myocardial cells, and 6.4 $\mu$S/$\mu$F for endocardial and epicardial cells. The output of the models was compared with independent experimental data for validation. 1-D simulations of a transmural ventricular fiber indicated that SK channel block may prolong the QT interval and increase the transmural dispersion of repolarization, potentially increasing the risk of arrhythmia in HF. Conclusion: Our results highlight the importance of considering the SK channels to improve the characterization of HF-induced ventricular remodeling. Simulations across various single-cell and 1-D scenarios suggest that pharmacological SK channel inhibition could lead to adverse effects in failing ventricles.**

***Index Terms*— Cardiac electrophysiological models, heart failure, human ventricle, SK channels.**

Manuscript submitted 27 June 2024. This work was supported by projects PID2022-139143OA-I00 and PID2022-140556OB-I00 funded by MICIU/AEI/10.13039/501100011033 and ERDF/EU, by project TED2021-130459B-I00 funded by MICIU/AEI/10.13039/501100011033 and NextGenerationEU/ PRTR and by Departamento de Ciencia, Universidad y Sociedad del Conocimiento, from Gobierno de Aragón (Spain) (Research Groups T71_23D and T39_23R)

Marta Gómez, Jesús Carro, and Violeta Monasterio are with Computing for Medical and Biological Applications Group, Universidad San Jorge, 50830, Villanueva de Gállego, Spain (e-mail: magomez@usj.es).

Esther Pueyo, Alba Pérez, and Aída Oliván are with Biomedical Signal Interpretation and Computational Simulation Group, Aragón Institute of Engineering Research (I3A), IIS Aragón, Universidad de Zaragoza, 50018 Zaragoza, Spain, and also with CIBER de Bioingeniería, Biomateriales y Nanomedicina (CIBER-BNN), 28029, Spain.

## I. Introduction

Heart failure (HF) is a condition characterized by the deterioration of the heart's electrical and contractile function, resulting from structural and functional remodeling. This leads to an inadequate pumping of blood, failing to meet the body's physiological and metabolic needs [1]. Often, HF is accompanied by other metabolic or cardiac pathologies, such as atrial fibrillation (AF), which is the most common arrhythmia in clinical practice [2]. Importantly, the presence of AF further increases the risk of mortality in HF patients with reduced ejection fraction [3].

The small conductance ($\sim$10 pS) calcium-activated potassium (SK) channels are an important group of potassium-selective ion channels that are garnering increasing attention in the field of cardiac electrophysiology as a promising anti-arrhythmic target in AF [4]. Unlike other ion channels, SK channels do not possess a voltage sensor; they are solely activated by calcium. SK channels are expressed in both human atria and ventricles, but the physiological and pathophysiological roles of SK channels are still poorly understood [5].

While the role of SK channels in cardiac tissue remains to be fully elucidated, it has been established that they are dormant in health and upregulated in diseased hearts [6]–[8]. In particular, in failing ventricular myocytes, SK channels may be upregulated and may present increased apparent $Ca^{2+}$ sensitivity, suggesting a relevant pathophysiological role in HF [9]. Notably, experimental observations have demonstrated that blocking SK channels leads to the prolongation of the ventricular action potential duration (APD) under HF conditions, while having no effect under physiological conditions [1]. These findings suggest that the upregulation of SK channels in pathological conditions could be an adaptive physiological response aimed at shortening the APD when the repolarization reserve is compromised [10]. Nevertheless, the precise conditions under which the action of these channels can be classified as pro-arrhythmic or anti-arrhythmic are still not thoroughly understood [11].

A powerful tool for understanding arrhythmias is the use of computational models of cardiac electrophysiology. In particular, action potential (AP) models of cardiac myocytes can be used to improve our understanding of cellular electrical function under physiological conditions or in response to

disease or drug-induced alterations [6]. While disease-specific models have been proposed to represent HF conditions in human ventricular cells [12], [13], these models lack an explicit characterization of the SK current. Thus, the objective of this study is to propose and validate a cellular model of ventricular electrophysiology that can facilitate the investigation of potential arrhythmogenecity stemming from the modulation of SK channels under HF conditions.

## II. Materials and Methods

### A. Experimental data for reference

Two previously published datasets were used for the development and validation of the HF model with incorporation of SK current formulation. To our best knowledge, these are the only available experimental studies on the effect of SK channel modulation in human failing ventricular myocytes. These datasets contain experimental measures of human ventricular AP variations under pharmacological SK channel blockade (*Blockade Dataset* [1]) and activation (*Activation Dataset* [14], [15]).

*1) Blockade Dataset (BD):* The first set of experimental data used in this work was published by Bonilla and coworkers in [1]. Full details are available in the original publication. In short, left ventricular mid-myocardial human myocytes were isolated from explanted end-stage failing hearts (n = 7 myocytes). APs were recorded in response to a train of 25 impulses at 0.5, 1 and 2 Hz at baseline and after apamin perfusion. The average of the last 10 cycles was used to calculate the APD at 50% and 90% of repolarization ($APD_{50}$ and $APD_{90}$). Three myocytes exhibiting late phase 3 early afterdepolarizations (EADs) after apamin infusion at 0.5 Hz were excluded from AP measurements. SK channel block with 100 nM apamin was found to prolong $APD_{50}$ and $APD_{90}$ at all rates.

From the original dataset, we calculated the relative change ($R$) in $APD_{50}$ and $APD_{90}$ induced by SK channel block, for 0.5 Hz, 1 Hz and 2 Hz pacing as

$$R = \frac{\mathrm{APD_{apamin}} - \mathrm{APD_{baseline}}}{\mathrm{APD_{baseline}}} 100, \tag{1}$$

where APD represents $APD_{50}$ or $APD_{90}$. The six resulting $R$ values (last column in Table II) were used as a reference for the adjustment of the maximal SK current conductance, as fully described in Section II-C.1.

*2) Activation Dataset (AD):* The second dataset used here contained experimental measurements from human left ventricular transmural biopsies and from papillary muscles and endocardial tissues ( [14], [15]) of HF patients, which were extracted by experienced cardiothoracic surgeons at Miguel Servet University Hospital. Mid-myocardial tissue slices were taken from the biopsies of 3 HF patients. Endocardial tissue slices were obtained from the papillary muscles and endocardial tissues of 23 HF patients. Upon collection, all tissues were submerged in cold Tyrode's solution (composition in mM: NaCl 140, KCl 6, CaCl2 1.8, MgCl2 (·6H2O), glucose 10, HEPES 10, BDM(2,3-butanedione monoxime) 30). Tissue slices of 350 $\mu$m thick were produced with a precision vibratome and were optically mapped after staining with RH237. $APD_{80}$ was measured at baseline and after addition of 100 $\mu$M SKA-31 (an SK-channel activator) from the voltage traces of both mid-myocardial (AD-mid) and endocardial tissue slices (AD-endo).

We calculated the relative decrement ($D$) in $APD_{80}$ induced by SK channel activation, for 0.5 Hz, 1 Hz and 2 Hz pacing as

$$D = \left| \frac{\mathrm{APD_{SKA\text{-}31}} - \mathrm{APD_{baseline}}}{\mathrm{APD_{baseline}}} 100 \right|, \tag{2}$$

where APD represents the median $APD_{80}$ over tissue slices for each pacing frequency. The three resulting $D$ values (last column in Table IV) were used as a reference for the estimation of the SKA-31 effect on the maximal SK current conductance, as fully described in Section II-C.2.

### B. Baseline cellular models

The O'Hara *et al.* model (ORd) [16], one of the most widely used and extensively tested models of a human ventricular myocyte, was selected to represent the electrophysiology of undiseased cells. In the original ORd model, we replaced the formulation of the fast sodium current, $I_{Na}$, with that of the ten Tusscher *et al.* model [17] to prevent propagation failure as proposed in [16]. Simulations with this model will be referred to as normal conditions (NC) from here on. The three versions of the model for epicardial, mid-myocardial and endocardial cells were used in the simulations, as indicated in subsequent sections.

The ORdmm model [18] was selected as starting point to simulate the electrophysiology of failing myocytes. The ORdmm model is a modified version of the original ORd model that represents the characteristic HF fenotype at the cellular level. HF-associated remodeling is introduced by applying scaling factors to maximal conductances and time constants of several ionic currents and fluxes. Full details can be found in the Supplementary material of the original article [18]. The ORdmm model is able to reproduce the $Ca^{2+}$ transients and abnormalities in $Ca^{2+}$ dynamics observed in failing human hearts, and has served as basis for simulation studies that have provided novel insights into the mechanisms behind HF-associated arrhythmogenicity [13], [18], [19]. Heterogeneous HF remodeling for endocardial, epicardial and mid-myocardial cells was implemented as in Gomez *et al.* [19]. In this work, we propose an extension of the ORdmm model to account for the effect of the SK channels as described next. We will refer to our new extended model as ORdmm-SK in subsequent sections.

### C. Formulation for the SK current, $I_{SK}$

To include $I_{SK}$ in the ORdmm-SK model, the formulation proposed in [20] was selected as a starting point:

$$I_{SK} = G_{SK} x_{SK} (V - E_K) \tag{3}$$

$$\frac{dx_{SK}}{dt} = \frac{x_{SK,\infty} - x_{SK}}{\tau_{SK}} \tag{4}$$

$$x_{SK,\infty} = \frac{1}{1 + (K_d / Ca_{SK})^n} \tag{5}$$

$$\tau_{SK} = \tau_0 + \frac{\tau_1}{1 + (Ca_{SK}/0.1)} \tag{6}$$

where $G_{SK}$ is the maximum conductance, $x_{SK}$ represents an activation gate with activation time constant $\tau_{SK}$, and $Ca_{SK}$ is the $Ca^{2+}$ concentration sensed by the SK channels. In Equation 6, the values of $\tau_0$ and $\tau_1$ were set to $\tau_0 = 4\,ms$ and $\tau_1 = 20\,ms$ as in [20], based on experimental patch clamp data. Since the formulation in [20] was proposed for undiseased ventricular cell models, the values of the parameters in Equation 5 were changed in the present study to $n = 3.14$, and $K_d = 0.345\,\mu M$, according to experimental evidence in human HF ventricular myocytes [21], to represent the augmented sensitivity for $Ca^{2+}$ of SK channels in HF. SK channels were set to sense $Ca^{2+}$ in the subsarcolemmal space, based on studies suggesting that L-Type $Ca^{2+}$ channels provide the immediate $Ca^{2+}$ microdomain for the activation of SK channels in cardiomyocytes [22], [23].

The value for conductance $G_{SK}$ was adjusted for the different cell types from experimental data as described in the following subsections.

*1) $G_{SK}$ adjustment for mid-myocardial cells:* For the mid-myocardial ORdmm-SK model, the maximal conductance $G_{SK}$ was adjusted so that the resulting model reproduced the experimental AP prolongation induced by $I_{SK}$ block in human ventricular failing myocytes (reference values from the BD dataset, presented in Table II). To do so, the optimal $G_{SK}$ value was determined by simulating the effect of apamin block under conditions resembling the experimental setup, and then minimizing the difference between the experimental (R) and the simulated changes (S) in $APD_{50}$ and $APD_{90}$. For the optimization, the following objective function was defined, based on the method described in [24]:

$$f(G_{SK}) = \sum_{i=1}^{6} (R_i - S_i(G_{SK}))^2, \tag{7}$$

where $R_i$ represents each of the six experimental reference values, while $S_i(G_{SK})$ represents the corresponding simulated change for a given conductance $G_{SK}$. To compute the $S_i$ values, the effect of apamin was simulated as complete SK channel block ($G_{SK} = 0$), since the concentration used in the experiments (i.e. 100 $nM$) was an order of magnitude higher than the IC50 value reported in the literature [25]. A total of 20 simulations were conducted with varying $G_{SK}$ values, ranging from 0 to 0.01 based on data from experimental reports [20]. The Brent's method was employed to search for the minimum of $f$ [26]. The value of $G_{SK}$ associated with the lowest error (minimum $f$) was finally selected.

Following the determination of the optimal $G_{SK}$ value, we proceeded to validate the extended mid-myocardial model against independent experimental data. Simulations were performed at pacing frequencies of 0.5, 1 and 2 Hz, and the resulting $APD_{80}$ was compared to experimental measures from the AD-mid dataset at baseline (Figure 3).

Additionally, we analyzed whether the extended model was able to reproduce the observations by Bonilla et al. [1] that $I_{SK}$ block induced EADs in several samples at slow pacing rates, while no EADs were observed at baseline. To do so, we conducted a sensitivity analysis to determine the influence of $I_{SK}$ on the generation of EADs at a low pacing rate of 0.5 Hz. Each conductance in the model was varied by $\pm 5\%$ and $\pm 10\%$ and the absence or presence of EADs was assessed both with and without $I_{SK}$ block. Finally, we carried out a similar sensitivity analysis to explore the influence of calcium-remodeling in the robustness of the adjustment (Supplementary materials, section S.1.).

*2) $G_{SK}$ adjustment for endocardial and epicardial cells:* Although experimental evidence is scarce, observations in human failing myocytes suggest that the distribution of $I_{SK}$ is transmurally heterogeneous, with the epicardial and the endocardial layers expressing a significantly higher $I_{SK}$ than the mid-myocardial layer [21]. Experimental evidence does not show significant differences between endocardial and epicardial cells ( [21]), so no independent adjustment was made for these two cell types and the same $G_{SK}$ value was assumed for both.

For the endocardial version of the extended model, the maximal conductance $G_{SK}$ was re-adjusted from the one found for the mid-myocardial cells so that the resulting model produced APD values within the range of the experimental values (AD-endo dataset at baseline). To do so, endocardial cells were simulated with increasing $G_{SK}$ values (between 100% and 200%) with respect to the baseline mid-myocardial model. Simulations were performed at pacing frequencies of 0.5, 1 and 2 Hz. Simulated APDs were compared to experimental measures at each frequency at baseline (dataset AD-endo at baseline). The maximum and minimum $G_{SK}$ values for which simulated $APD_{80}$ matched the experimental ranges at all frequencies were determined. The midpoint of the resulting $G_{SK}$ range was finally selected (Figure 5).

Following the re-adjustment of the optimal $G_{SK}$ value, we proceeded to compare the extended endocardial model's output against experimental data from the AD-endo dataset with SKA 31 activation, as follows. First, the effect of SKA-31 was incorporated in the models as a scale factor modulating $G_{SK}$, with the amount of upregulation being equal for all cell types. To do so, a suitable value for the scale factor was estimated by performing simulations with the mid-myocardial extended model and comparing the results with the experimental values in the AD-mid dataset with SKA 31 activation (Table IV). Using the same adjustment methodology as in section II-C.1, a 165% $G_{SK}$ increase was estimated to reproduce the experimental $APD_{80}$ decrease induced by SKA-31 activation. Then, that scale factor was introduced in the endocardial model to simulate SK channel activation, and the resulting APD values were compared to experimental values from the dataset AD-endo under SKA-31 activation (Figure 7).

### D. Transmural fiber model

A one-dimensional model of ventricular tissue was used to investigate the effects of SK channel modulation in two markers of ventricular arrhythmic risk: the transmural dispersion of repolarization (TDR) and the QT interval prolongation as derived from the pseudo-ECG. To simulate the electrical activity of a transmural wedge preparation, we generated a 1.70 cm-long fiber composed of 0.60 cm, 0.45 cm, and 0.65 cm of endocardial, mid-myocardial and epicardial cells respectively. Normal conditions (NC), failing conditions (FC) and failing conditions with 100% $I_{SK}$ block (FCB) were compared. The fiber was discretized with $\Delta x$ = 0.01 cm. The diffusion coefficient was set to D = 0.06 mm$^2$/ms (NC) and D = 0.03 mm$^2$/ms (FC) [19] resulting in conduction velocity values of 50 cm/s in NC and 22.5 cm/s in FC. Stimuli were applied every 1000 ms until reaching steady state. Table I shows a summary of the conditions used in each situation.

TABLE I
SIMULATION PARAMETERS FOR THE 1D TRANSMURAL MODEL

| | NC | FC | FCB |
|---|---|---|---|
| Cell model | ORd | ORdmm-SK | ORdmm-SK |
| $I_{SK}$ modulation | — | $G_{SK}^{epi}$=6.4 $\mu$S/$\mu$F<br>$G_{SK}^{mid}$=4.288 $\mu$S/$\mu$F<br>$G_{SK}^{endo}$=6.4 $\mu$S/$\mu$F | $G_{SK}^{epi}$=0<br>$G_{SK}^{mid}$=0<br>$G_{SK}^{endo}$=0 |
| Diffusion coefficient | D=0.06 $mm^2$/ms | D=0.03 $mm^2$/ms | D=0.03 $mm^2$/ms |

Repolarization time (RT) and transmural dispersion of repolarization (TDR) were computed as in [19]. In short, $APD_{90}$ was computed for all cells between positions 0.15 cm to 1.55 cm in the strand, to avoid border effects. Then, RT for each cell was computed as the sum of $APD_{90}$ plus the time needed by the wavefront to reach that cell. TDR was computed as the difference between the maximum and the minimum RT along the fiber. Finally, the QT intervals were measured in pseudo-ECGs, computed as the extracellular potential ($\Phi$) recorded by an electrode placed 1.7 cm away from the epicardial end of the fiber, in the fiber direction.

### E. Numerical simulations

Cell simulations were performed using the software DENIS [27], a cardiac electrophysiology simulator based on the CellML standard. Fiber simulations were implemented in FORTRAN and were run using the software ELVIRA [28]. In both cases, Forward Euler method was used for numerical integration with a time step of $0.002\,ms$. Models were stimulated with monophasic current pulses with an amplitude corresponding to twice the diastolic threshold (80 $\mu A/\mu F$ for cell and 248 $\mu A/\mu F$ for tissue), except for single-cell simulations that were compared to experimental data from tissue, where an adapted biphasic stimulation waveform was applied [29]. Models were paced for 600 cycles to ensure a state of equilibrium. After steady-state was reached, 20 cycles were simulated in all cases.

## III. RESULTS

### A. Updated model for failing mid-myocardial cells

For the mid-myocardial ORdmm-SK model, as a result of the adjustment process, the optimal value for the SK current conductance was found to be $G_{SK}^{mid}$ = 4.288 $\mu$S/$\mu$F. The extended model produced average prolongations of 23% for $APD_{50}$ and 21% for $APD_{90}$ after $I_{SK}$ block, in range with the reference average prolongations of 22% for $APD_{50}$ and 24% for $APD_{90}$. Simulated and experimental relative changes are summarized in Table II. Simulated AP traces at 0.5, 1 and 2 Hz are depicted in Figure 1, both with and without $I_{SK}$ block. Figure 2 depicts the $I_{SK}$ traces, together with the underlying $[Ca^{2+}]_{ss}$ transients, at different stimulation frequencies. Supplementary figures S9 to S24 show a comparison of current traces between ORdmm and ORdmm-SK.

TABLE II
MID-MYOCARDIAL CELLS: RELATIVE $APD_{50}$ AND $APD_{90}$ PROLONGATION INDUCED BY $I_{SK}$ BLOCK AT DIFFERENT PACING FREQUENCIES

| APD marker | Frequency | Prolongation | |
|---|---|---|---|
| | | Simulated | Reference ($R$) |
| $APD_{50}$ | 0.5 Hz | 21.91% | 22.68% |
| | 1 Hz | 25.39% | 26.33% |
| | 2 Hz | 22.16% | 15.15% |
| $APD_{90}$ | 0.5 Hz | 18.05% | 33.19% |
| | 1 Hz | 21.44% | 22.73% |
| | 2 Hz | 22.26% | 17.25% |

Upon comparison with independent experimental data (AD-mid measurements at baseline), the new ORdmm-SK model rendered $APD_{80}$ values within the limits of experimental measurements at all frequencies (Figure 3). Statistical analysis based on tolerance intervals confirmed the match (see Supplementary materials, section S.2.). For illustration, results with the initial failing myocyte model (ORdmm) were also included in the comparison.

In relation to the sensitivity analysis, the introduction of variability in ionic currents other than $I_{SK}$ did not yield observable EADs at any pacing frequency in case of active SK channels. However, in subsequent simulations under $I_{SK}$ block, EADs were found for reduced $I_{Kr}$in every cycle, and for augmented $I_{NaL}$ and $I_{CaL}$ in one out of every two cycles (Table III). Figure 4 shows examples of EAD traces.

TABLE III
EAD DEVELOPMENT (DARK GREY) UNDER IONIC CURRENT VARIATIONS AND $I_{SK}$ BLOCK ($G_{SK} = 0$). VALUES INDICATE PERCENTAGE OF AP WITH EADS.

| | $I_{Kr}$ | $I_{NaL}$ | $I_{CaL}$ |
|---|---|---|---|
| -10% | 100% | | |
| -5% | 100% | | |
| +5% | | | |
| +10% | | 50% | 50% |

### B. Updated model for failing endocardial cells

For the endocardial ORdmm-SK model, a range of suitable $G_{SK}$ values spanning from 4.288 $\mu$S/$\mu$F to 8.654 $\mu$S/$\mu$F was identified. The final $G_{SK}$ value was selected as the midpoint

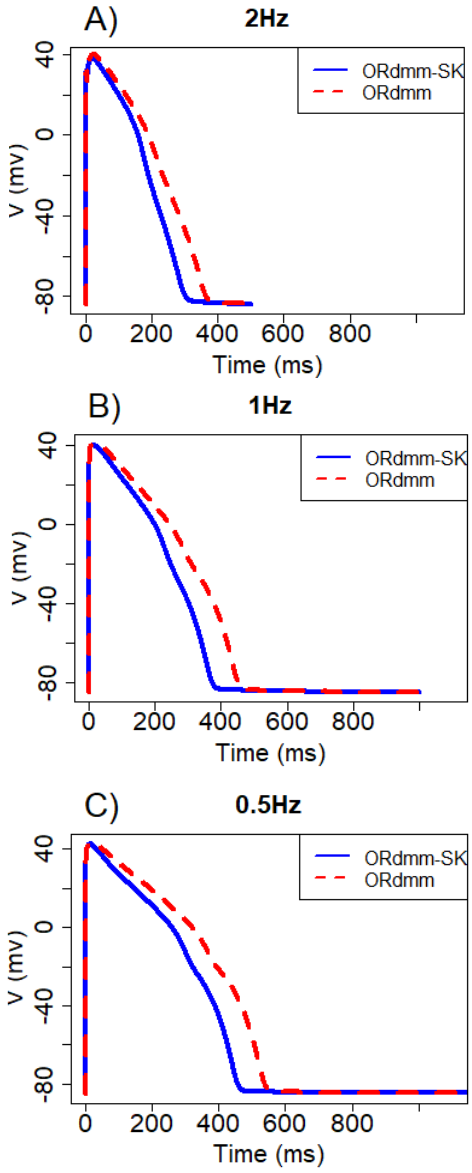


Fig. 1. Simulated APs with and without $I_{SK}$ block at pacing frequencies of (A) 2 Hz, (B) 1 Hz and (C) 0.5 Hz for mid-myocardial cells.

of this range, specifically 6.471$\mu$S/$\mu$F. This value was 1.51 times higher than in mid-myocardial cells. Figure 5 depicts the output of the adjusted endocardial model with respect to the original experimental data and simulated AP traces at 0.5, 1 and 2 Hz are presented in Figure 6, both with and without $I_{SK}$ block.

Upon comparison with independent experimental data (AD-endo measurements with SKA-31 activation), the new ORdmm-SK model rendered $APD_{80}$ values within the limits of experimental measurements at all frequencies (Figure 7).

### *C. Effects of $I_{SK}$ block on repolarization heterogeneity*

Simulations with the transmural fiber model showed that failing conditions (FC) increased both TDR and the QT interval with respect to NC, and that subsequent $I_{SK}$ block

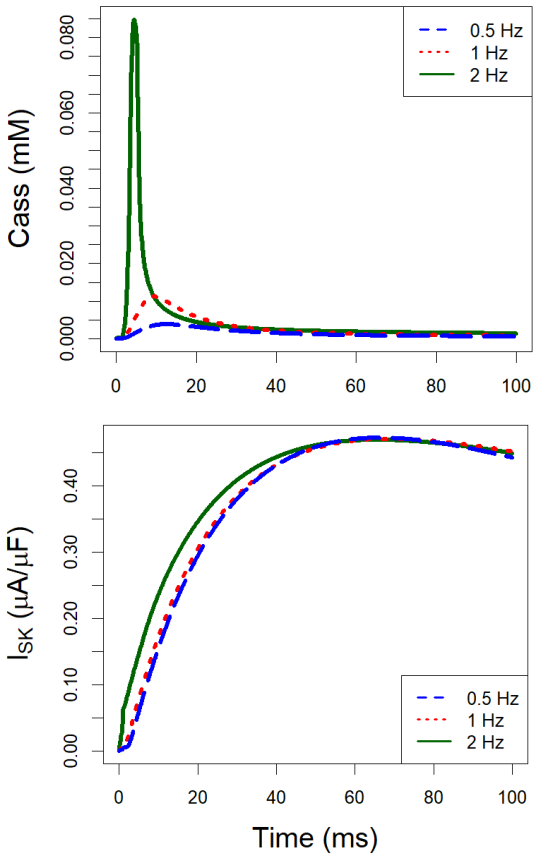


Fig. 2. Simulated $[Ca^{2+}]_{ss}$ transients and $I_{SK}$ traces at different pacing frequencies for mid-myocardial cells.

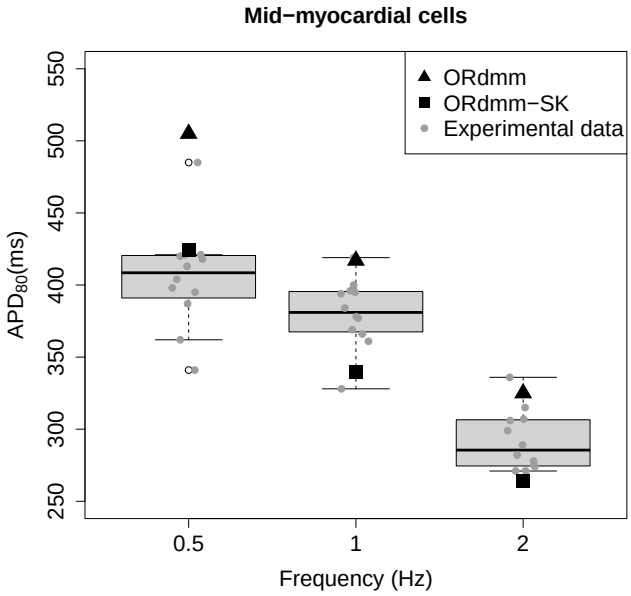


Fig. 3. The distribution of gray dots represents the experimental AD-mid dataset at baseline ($APD_{80}$ of myocardial cells) at three different stimulation frequencies: 0.5, 1 and 2 Hz. Experimental data are compared with simulated data from the new model with SK channels (ORdmm-SK) and the model with $I_{SK}$ block (ORdmm) in mid-myocardial cells.

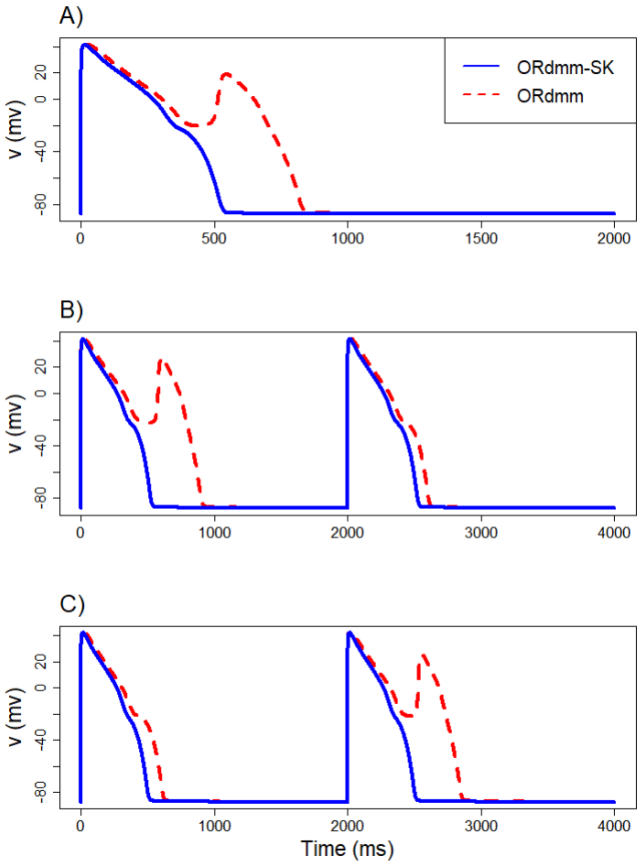


Fig. 4. Simulated APs with (dashed line) and without (straight line) $I_{SK}$ block at pacing frequency of 0.5 Hz. Under $I_{SK}$ block, EADs developed for variations of: (A) 5% decrease in $I_{Kr}$, (B) 10 % increase in $I_{NaL}$ and (C) 10 % increase in $I_{CaL}$.

TABLE IV
MID-MYOCARDIAL CELLS: EXPERIMENTAL DECREMENT IN $APD_{80}$ INDUCED BY $I_{SK}$ PHARMACOLOGICAL ACTIVATION AT DIFFERENT PACING FREQUENCIES

| APD marker | Frenquency | Prolongation |
|---|---|---|
| | | Reference ($D$) |
| $APD_{80}$ | 0.5 Hz | 15.12% |
| | 1 Hz | 13.05% |
| | 2 Hz | 5.21% |

(FCB) produced substantial additional increases in both markers (Figure 8).

## IV. DISCUSSION

The pathophysiological role of SK channels in ventricular electrophysiology remains to be fully characterized. In HF, experimental studies have found significant differences in SK channel expression and regulation with respect to healthy ventricular myocytes. For example, in human ventricular tissue, increased SK expression has been reported at mRNA [11] and protein level [21], and pharmacological SK modulation has been found to influence APD [1], [14]. According to our study, the inclusion of the SK current in an electrophysiological model of a ventricular myocyte improves the characterization of the electrophysiological remodeling observed in HF.

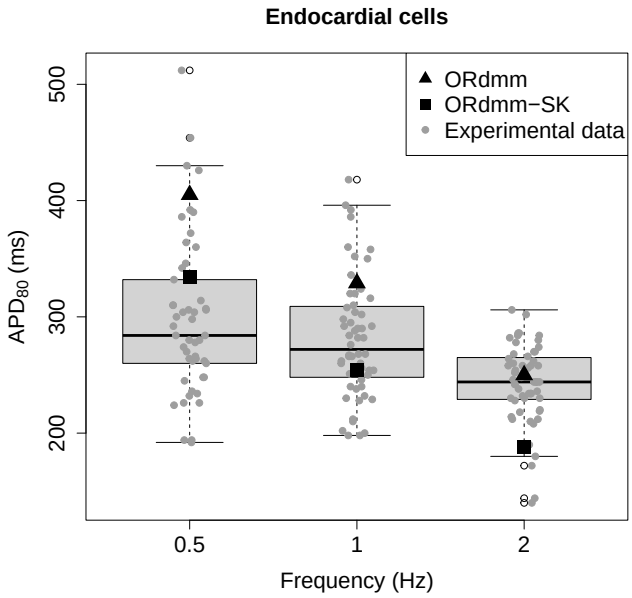


Fig. 5. The distribution of gray dots represents the experimental AD-endo dataset at baseline ($APD_{80}$ of endocardial cells) at three different stimulation frequencies: 0.5, 1 and 2 Hz. Experimental data are compared with simulated data from the new model with SK channels (ORdmm-SK) and the model with $I_{SK}$ block (ORdmm) in endocardial cells.

This updated model enables further investigation into the proarrhythmic or antiarrhythmic effects of pharmacological interventions targeting SK channels in HF conditions.

The updated model proposed in this study extends an existing HF-specific ventricular electrophysiological model (ORdmm) by incorporating an adjusted formulation for $I_{SK}$. For mid-myocardial myocytes, the updated model was adjusted to replicate apamin-induced APD variations observed experimentally in human failing myocytes (see Table II) across various pacing frequencies. Simulated and experimental APD variations were most similar at 1 Hz pacing, while the highest discrepancy was observed in $APD_{90}$ at 0.5 Hz, where the variation in the reference data exceeded our model's prediction. However, it is worth to note the small sample size for 0.5 Hz data, given that 3 out of 7 samples exhibited EADs after apamin perfusion, and those recordings with EADs were excluded from APD calculations [1]. At different stimulation rates, although the $Ca^{2+}$ transient was significantly different (being higher and narrower at higher frequencies), the $I_{SK}$ current did not vary considerably. The main reason for this is that the $Ca^{2+}$ concentration far exceeded the required threshold for activation. An additional factor could be that, at short pacing cycle lengths, SK channels would be rapidly activated by elevated $Ca^{2+}$, while at long pacing cycle lengths, long $Ca^{2+}$ transient duration with persistent transsarcolemmal $Ca^{2+}$ influx through L-type $Ca^{2+}$ channels may also facilitate activation of SK channels, as has been pointed out in the literature [30].

To account for the reported transmural variance in SK channel modulation [21], we re-adjusted the maximal conductance of $I_{SK}$ for the endocardial cell model. This adjustment yielded

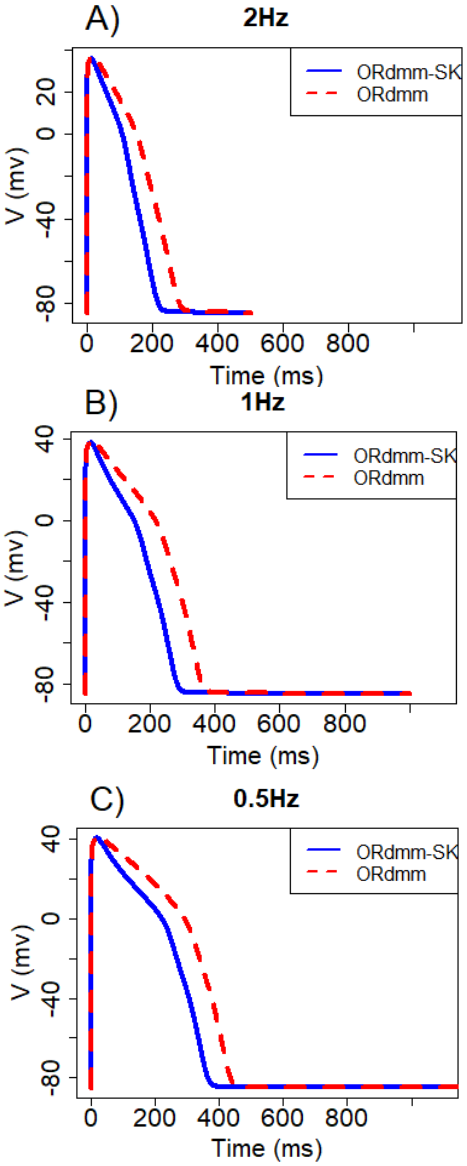


Fig. 6. Simulated APs with and without $I_{SK}$ block at pacing frequencies of (A) 2 Hz, (B) 1 Hz and (C) 0.5 Hz for endocardial cells.

a $G_{SK}$ value 1.51 times greater than in the mid-myocardial case. Given the absence of experimental data for additional adjustments, the remaining parameters in the $I_{SK}$ formulation were left unchanged with respect to the mid-myocardial model. Nonetheless, the adjusted endocardial model produced $APD_{90}$ values well within the range of the reference experimental measurements in human failing endocardial myocytes (see Figure 5).

For mid-myocardial cells, the updated model yielded $APD_{80}$ values in good agreement with experimental ranges from the AD-mid dataset at different pacing rates (Figure 3). At slow pacing rates (0.5 Hz), EADs appeared under $I_{SK}$ block in several variations of the model (Table III), which is consistent with observations from Bonilla et al. [1], who reported frequent EADs after apamin infusion but no EADs at baseline in mid-myocardium failing ventricular cells. Our

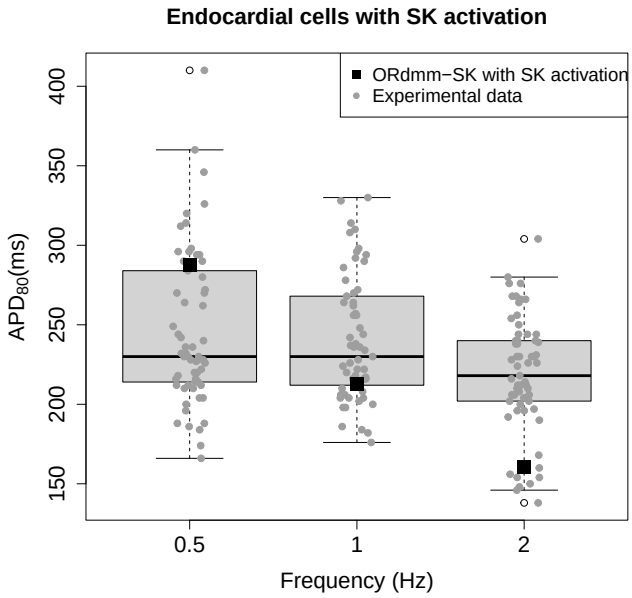


Fig. 7. The distribution of gray dots represents the experimental AD-endo dataset with activator ($APD_{80}$ of endocardial cells) at three different stimulation frequencies: 0.5, 1 and 2 Hz. Experimental data are compared with simulated data from the new model with SK channels (ORdmm-SK) with $I_{SK}$ activation in endocardial cells.

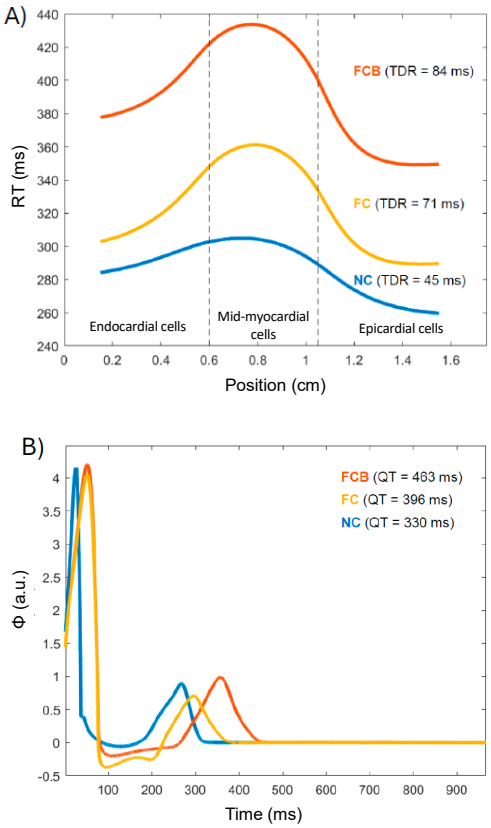


Fig. 8. A) Repolarization time in normal (NC), failing (FC) and failing with $I_{SK}$ block (FCB) conditions. B) Pseudo-ECG in normal (NC), failing (FC) and failing with $I_{SK}$ block (FCB) conditions.

simulations suggest that, at low pacing rates, SK channels may exert an antiarrhythmic effect by compensating for the low repolarization reserve in failing ventricles, which is in line with experimental literature [21], [31]. In endocardial cells, pharmacological activation of SK channels led to substantial APD shortening, yielding $APD_{80}$ values within the range of independent experimental observations (Figure 7).

Having validated the updated model in those scenarios, we conducted a proof-of-concept study to highlight the importance of investigating the proarrhythmic effects of SK channel modulation in failing ventricles. SK channels have been proposed as a potential target for treating atrial fibrillation [9]. Initially, research primarily focused on the pharmacological effects of SK modulation within atrial electrophysiology, assuming $I_{SK}$ played a minor role in ventricular function [32], [33]. However, as our tissue simulations illustrate, $I_{SK}$ inhibition may have proarrhythmic effects under failing conditions. In our simulations, SK channel block increased transmural dispersion of repolarization and induced QT prolongation, two manifestations that are considered to be predisposing factors for ventricular arrhythmias. Therefore, our *in silico* predictions support the notion that SK channel modulators may have limited utility in treating atrial fibrillation in failing hearts. This view is consistent with experimental literature questioning the role of SK channels as atria-selective drug targets [11].

Our study has some limitations that should be considered for future research. In the $I_{SK}$ formulation, we opted for a linear current-voltage relationship, in line with the weak rectification observed in some experimental studies [22], [34]. However, more complex rectification kinetics in SK currents has also been reported in the literature [35]. Future research could explore enhancing the $I_{SK}$ formulation by incorporating additional rectification parameters. Other limitation of this work is the use of relative APD prolongation instead of the absolute value for model calibration. It is known that the degree of APD prolongation in response to inhibition of a repolarizing current depends on the initial APD [36]. In our study, however, the APD simulated with the ORdmm model was notably higher than the experimental measurements used as reference [1]. Therefore, using absolute APD values for the $G_{SK}$ adjustment would have required a previous readjustment of the ORdmm model to fit the experimental data. Since that approach would preclude comparisons with previous in-silico studies [19], we opted for using relative values, thus allowing the evaluation of the isolated effect of $I_{SK}$ inclusion in the model.

While keeping the ORdmm model as the foundation for our research allowed a direct comparison with previous studies, other models derived from ORd have been proposed in recent years. Having established that including the $I_{SK}$ current is crucial for modeling failure conditions, future research could focus on adapting the SK channel formulation for integration into the ventricular model ToR_ORd [37], which represents an update of the ORd model including, among others, modifications to the $I_{Ca,L}$ current and thus the calcium dynamics. For such adaptation, it will be necessary consider the presence of SK channels in the different cell compartments, since $I_{Ca,L}$ channels are not limited to the subsarcolemmal space in the ToR_ORd model. In our work, as a first approximation, SK channels were assumed to be colocalized with L-type $Ca^{2+}$ channels in the subsarcolemmal compartment; further research could investigate the influence of the subcellular localization of SK channels on AP morphology and APD dynamics.

Regarding the 1-D simulations, we retained the transmurality representation from previous studies [19]. While the behaviour of mid-myocardial cells is controversial [38], [39], the experimental data used for reference in this study presented a higher median APD value for mid-myocardial cells than for endocardial cells, and the adjusted models were calibrated to match the experimental ranges. It is to note, however, that a single cell model is meant to represent an instance from a diverse population. Further research on the role of SK channels could adopt a population-of-models approach such that the derived insights can be a more realistic reflection of electrophysiological variability. Also, it is important to note that in the transmural fiber model we chose the same value for the maximal SK conductance for both epicardial and endocardial cells. This decision was due to the lack of additional experimental data that would allow for distinct adjustments for epicardial cells. Therefore, our quantitative results on TDR and QT variations should only be considered as exploratory, since they are dependent on the interplay between the effects of SK modulation in the different layers. Despite this limitation, our findings emphasize the importance of considering ventricular SK channel activity to accurately characterize pro-arrhythmic mechanisms induced by HF.

## V. Conclusion

Our research introduces an updated computational cell model for representing human ventricular electrophysiology in HF conditions. By incorporating $I_{SK}$ into the model, we have highlighted the importance of considering the SK channels to improve the characterization of HF-induced remodeling. Our simulations across various scenarios provide evidence suggesting that pharmacological SK channel inhibition could lead to adverse effects in failing ventricles.

## References

[1] I. M. Bonilla, V. P. Long, P. Vargas-Pinto, P. Wright, A. Belevych, Q. Lou, K. Mowrey, J. Yoo, P. F. Binkley, V. V. Fedorov, S. Györke, P. M. Janssen, A. Kilic, P. J. Mohler, and C. A. Carnes, "Calcium-activated potassium current modulates ventricular repolarization in chronic heart failure," *PLoS ONE,*, vol. 9, no. 10, pp. 1–11, 2014.

[2] W. Kannel, P. Wolf, E. Benjamin, and D. Levy, "Prevalence, incidence, prognosis, and predisposing conditions for atrial fibrillation: population-based estimates," *Am J Cardiol*, vol. 82, pp. 2–9, 1998.

[3] T. Wang, M. Larson, D. Levy, R. Vasan, E. Leip, P. Wolf, R. D'Agostino, J. Murabito, W. Kannel, and E. Benjamin, "Temporal relations of atrial fibrillation and congestive heart failure and their joint influence on mortality: the framingham heart study," *Circulation 107*, vol. 107, no. 25, pp. 2920–2925, 2003.

[4] J. Heijman, X. Zhou, S. Morotti, C. E. Molina, I. H. Abu-Taha, M. Tekook, T. Jespersen, Y. Zhang, S. Dobrev, H. Milting, J. Gummert, M. Karck, M. Kamler, A. El-Armouche, A. Saljic, E. Grandi, S. Nattel, and D. Dobrev, "Enhanced $Ca^{2+}$-Dependent SK-Channel Gating and Membrane Trafficking in Human Atrial Fibrillation," *Circulation Research*, vol. 132, no. 9, pp. 116–133, 2023.

[5] T. Liu, T. Li, D. Xu, Y. Wang, Y. Zhou, J. Wan, C. L.-H. Huang, and X. Tan, "Small-conductance calcium-activated potassium channels in the heart: expression, regulation and pathological implications," *Philosophical Transactions of the Royal Society B: Biological Sciences,*, vol. 378, no. 1879, 2023.

[6] A. Varró, J. Tomek, N. Nagy, L. Virág, E. Passini, B. Rodriguez, and I. Baczkó, "Cardiac transmembrane ion channels and action potentials: cellular physiology and arrhythmogenic behavior," *Physiological Reviews*, vol. 101, no. 3, pp. 1083–1176, 2021.

[7] D. Terentyev, A. E. Belevych, B.-R. Choi, and S. Hamilton, "To block or not to block: Targeting sk channels in diseased hearts," *Journal of Molecular and Cellular Cardiology*, vol. 183, pp. 98–99, 10 2023. doi: 10.1016/j.yjmcc.2023.09.005.

[8] A. Giommi, A. R. B. Gurgel, G. L. Smith, and A. J. Workman, "Does the small conductance ca2+-activated k+ current isk flow under physiological conditions in rabbit and human atrial isolated cardiomyocytes?," *Journal of Molecular and Cellular Cardiology*, vol. 183, pp. 70–80, 10 2023. doi: 10.1016/j.yjmcc.2023.09.002.

[9] X. D. Zhang, P. N. Thai, D. K. Lieu, and N. Chiamvimonvat, "Cardiac small-conductance calcium-activated potassium channels in health and disease," *Pflügers Archiv - European Journal of Physiology*, vol. 473, no. 3, pp. 477–489, 2021.

[10] M. Gu, Y. Zhu, X. Yin, and D.-M. Zhang, "Small-conductance $Ca^{2+}$-activated $K^+$ channels: insights into their roles in cardiovascular disease," *Experimental & molecular medicine*, vol. 50, no. 4, pp. 1–7, 2018.

[11] E. Darkow, T. T. Nguyen, M. Stolina, F. A. Kari, C. Schmidt, F. Wiedmann, I. Baczkó, P. Kohl, S. Rajamani, U. Ravens, and R. Peyronnet, "Small Conductance $Ca^{2+}$-Activated $K^+$ (SK) Channel mRNA Expression in Human Atrial and Ventricular Tissue: Comparison Between Donor, Atrial Fibrillation and Heart Failure Tissue," *Frontiers in Physiology*, vol. 12, pp. 1–16, 2021.

[12] M. M. Elshrif, P. Shi, and E. M. Cherry, "Representing variability and transmural differences in a model of human heart failure," *IEEE Journal of Biomedical and Health Informatics*, vol. 19, no. 4, pp. 1308–1320, 2015.

[13] J. F. Gomez, K. Cardona, and B. Trenor, "Lessons learned from multiscale modeling of the failing heart," *Journal of Molecular and Cellular Cardiology*, vol. 89, pp. 146–159, 2015.

[14] A. Pérez, L. García, M. Lopez, F. Mancebon, A. Vaca, C. Ballester, M. Pérez, R. Kohler, E. Pueyo, and A. Oliván, "SK channels contribution to ventricular electrophysiology in heart failure patients," *Cardiovascular Research*, vol. 118, 2022.

[15] A. Oliván-Viguera, A. Pérez-Martínez, L. García-Mendivil, A. S. Vaca-Nuñez, J. A. Bellido-Morales, J. F. Sorribas-Berjón, M. Matamala-Adell, M. Vázquez-Sancho, J. Fañanás-Mastral, J. M. Vallejo-Gil, C. Ballester-Cuenca, and E. Pueyo, "Eletrophysiological and immunohistological evaluation of SK channels from human ventricles: differential functional expression in valvular disease," in *47th EWGCCE Annual meeting of the ESC Working Group on Cardiac Cellular Electrophysiology*, (Copenhagen, Dennmark), 2023.

[16] T. O'Hara, L. Virág, A. Varró, and Y. Rudy, "Simulation of the undiseased human cardiac ventricular action potential: Model formulation and experimental validation," *PLoS Computational Biology*, vol. 7, no. 5, 2011.

[17] K. H. W. J. ten Tusscher, D. Noble, P. J. Noble, and a. V. Panfilov, "A model for human ventricular tissue," *American journal of physiology. Heart and circulatory physiology*, vol. 286, no. 4, pp. 573–1589, 2004.

[18] M. T. Mora, J. M. Ferrero, L. Romero, and B. Trenor, "Sensitivity analysis revealing the effect of modulating ionic mechanisms on calcium dynamics in simulated human heart failure," *PLOS ONE*, vol. 12, no. 11, 2017.

[19] J. F. Gomez, K. Cardona, L. Romero, J. M. Ferrero, and B. Trenor, "Electrophysiological and structural remodeling in heart failure modulate arrhythmogenesis. 1D simulation study," *PLoS ONE*, vol. 9, no. 9, 2014.

[20] J. Landaw, Z. Zhang, Z. Song, M. B. Liu, R. Olcese, P. S. Chen, J. N. Weiss, and Z. Qu, "Small-conductance $Ca^{2+}$-activated $K^+$ channels promote J-wave syndrome and phase 2 reentry," *Heart Rhythm*, vol. 17, no. 9, pp. 1582–1590, 2020.

[21] P. C. Chang, I. Turker, J. C. Lopshire, S. Masroor, B. L. Nguyen, W. Tao, M. Rubart, P. S. Chen, Z. Chen, and T. Ai, "Heterogeneous upregulation of apamin-sensitive potassium currents in failing human ventricles," *Journal of the American Heart Association*, vol. 2, no. 1, pp. 1–9, 2013.

[22] L. Lu, Q. Zhang, V. Timofeyev, Z. Zhang, J. Young, H. Shin, A. Knowlton, and C. N., "Molecular coupling of a $Ca^{2+}$-activated $K^+$ channel to L-type $Ca^{2+}$ channels via alpha-actinin-2," *Circ Research*, vol. 100, no. 1, pp. 112–120, 2007.

[23] X. Zhang, Z. Coulibaly, W. Chen, H. Ledford, J. Han Lee, P. Sirish, G. Dai, Z. Jian, F. Chuang, I. Brust-Mascher, E. Yamoah, Y. Chen-Izu, L. Izu, and N. Chiamvimonvat, "Coupling of SK channels, L-type $Ca^{2+}$ channels, and ryanodine receptors in cardiomyocytes," *Scientific Reports*, vol. 8, no. 1, 2018.

[24] J. Carro, E. Pueyo, and J. F. Rodríguez Matas, "A response surface optimization approach to adjust ionic current conductances of cardiac electrophysiological models. application to the study of potassium level changes," *PloS one*, vol. 13, no. 10, 2018.

[25] D. C. H. Benton, M. Garbarg, and G. W. J. Moss, "The Relationship between Functional Inhibition and Binding for K(Ca)2 Channel Blockers," *PLoS ONE*, vol. 8, no. 9, 2013.

[26] R. Brent, "Algorithms for minimization without derivatives," *Ann Biomed Eng*.

[27] V. Monasterio, J. Castro-Mur, and J. Carro, "Denis: Solving cardiac electrophysiological simulations with volunteer computing," *PLoS ONE*, vol. 13, no. 10, 2018.

[28] H. E., F. J.M., D. M., and R. J.F., "Adaptive macro finite elements for the numerical solution of monodomain equations in cardiac electrophysiology," *Ann Biomed Eng*, vol. 38, no. 7, p. 2331–2345, 2010.

[29] V. Monasterio, E. Pueyo, J. F. Rodríguez-Matas, and J. Carro, "Cardiac cells stimulated with an axial current-like waveform reproduce electrophysiological properties of tissue fibers," *Computer Methods and Programs in Biomedicine*, vol. 226, 2022.

[30] P.-C. Chang and P.-S. Chen, "Sk channels and ventricular arrhythmias in heart failure," *Trends in cardiovascular medicine*, vol. 25, no. 6, pp. 508–14, 2015.

[31] S.-K. Chua, P.-c. Chang, M. Maruyama, I. Turker, T. Shinohara, M. J. Shen, Z. Chen, C. Shen, M. Rubart-von der Lohe, J. C. Lopshire, M. Ogawa, J. N. Weiss, S.-F. Lin, T. Ai, and P.-S. Chen, "Small-Conductance Calcium-Activated Potassium Channel and Recurrent Ventricular Fibrillation in Failing Rabbit Ventricles," *Circulation research*, vol. 108, no. 8, pp. pp. 971–979, 2011.

[32] N. S., "Calcium-activated potassium current: a novel ion channel candidate in atrial fibrillation," *J Physiol*, vol. 587, pp. 1385–1386, 2009.

[33] J. Diness, B. Bentzen, U. Sorensen, and M. Grunnet, "Role of calcium-activated potassium channels in atrial fibrillation pathophysiology and therapy," *J Cardiovasc Pharmaco*, vol. 66, no. 5, pp. 441–448, 2015.

[34] Q. Zhang, V. Timofeyev, L. Lu, N. Li, A. Singapuri, M. Long, C. Bond, J. Adelman, and N. Chiamvimonvat, "Functional roles of a $Ca^{2+}$-activated $K^+$ channel in atrioventricular nodes," *Circ Research*, vol. 102, no. 4, pp. 465–471, 2008.

[35] P. Bronk, T. Y. Kim, I. Polina, S. Hamilton, R. Terentyeva, K. Roder, G. Koren, D. Terentyev, and B.-R. Choi, "Impact of $I_{SK}$ Voltage and $Ca^{2+}$/$Mg^{2+}$-Dependent Rectification on Cardiac Repolarization," *Biophysical journal*, vol. 119, no. 3, pp. 690–704, 2020.

[36] W. Yamamoto, K. Asakura, H. Ando, T. Taniguchi, A. Ojima, T. Uda, T. Osada, S. Hayashi, C. Kasai, N. Miyamoto, H. Tashibu, T. Yoshinaga, D. Yamazaki, A. Sugiyama, Y. Kanda, K. Sawada, and Y. Sekino, "Electrophysiological characteristics of human ipsc-derived cardiomyocytes for the assessment of drug-induced proarrhythmic potential," *PLoS ONE*, 11 2016.

[37] J. Tomek, A. Bueno-Orovio, E. Passini, X. Zhou, A. Minchole, O. Britton, C. Bartolucci, S. Severi, A. Shrier, L. Virag, A. Varro, and B. Rodriguez, "Development, calibration, and validation of a novel human ventricular myocyte model in health, disease, and drug block," *eLife*, vol. 8, p. e48890, dec 2019.

[38] C. Antzelevitch, "M cells in the human heart," *Circulation research*, vol. 106, no. 5, pp. 815–817, 2010.

[39] A. V. Glukhov, V. V. Fedorov, Q. Lou, V. K. Ravikumar, P. W. Kalish, R. B. Schuessler, N. Moazami, and I. R. Efimov, "Transmural dispersion of repolarization in failing and nonfailing human ventricle," *Circulation research*, vol. 106, no. 5, pp. 981–991, 2010.